JRSM Cardiovascular Disease

Diagnostic Performance of Virtual Fractional Flow Reserve derived from routine Coronary Angiography using Segmentation Free Reduced order (1-Dimensional) Flow Modelling

Journal:	*JRSM Cardiovascular Disease*
Manuscript ID	CVD-20-045
Manuscript Type:	Research Paper
Date Submitted by the Author:	28-Aug-2020
Complete List of Authors:	MOHEE, KEVIN; Swansea Bay University Health Board, Department of Cardiology Mynard, Jonathan; The University of Melbourne - Parkville Campus, Department of Cardiology, Royal Children's Hospital Dhunnoo, Gauravsingh; Swansea Bay University Health Board, Department of Cardiology Davies, Rhodri; Swansea Bay University Health Board Nithiarasu, Perumal; Swansea University School of Engineering, Biomedical Engineering Group, Zienkiewicz Centre for Computational Engineering, College of Engineering Halcox, Julian; Swansea University Medical School Obaid, Daniel ; Swansea University Medical School
Keywords:	Coronary imaging: angiography / ultrasound / Doppler / CC < Diagnostic Testing < Cardiology, Catheter-based coronary interventions: stents < Treatment < Cardiology, Cardiovascular imaging agents / techniques < Diagnostic Testing < Cardiology
Abstract:	Introduction: Fractional flow reserve (FFR) improves assessment of the physiological significance of coronary lesions compared with conventional angiography. However, it is an invasive investigation. We tested the performance of a virtual FFR (1D-vFFR) using routine angiographic images and a rapidly performed reduced order computational model. Methods: Quantitative coronary angiography (QCA) was performed in 102 with coronary lesions assessed by invasive FFR. A 1D-vFFR for each lesion was created using reduced order (one-dimensional) computational flow modelling derived from conventional angiographic images and patient specific estimates of coronary flow. The diagnostic accuracy of 1D-vFFR and QCA derived stenosis was compared against the gold standard of invasive FFR using area under the receiver operator characteristic curve (AUC). Results: QCA revealed the mean coronary stenosis diameter was 44% ± 12% and lesion length 13 ± 7 mm. Following angiography calculation of the 1D-vFFR took less than one minute. Coronary stenosis (QCA) had a

	significant but weak correlation with FFR (r=-0.2, p= 0.04) and poor diagnostic performance to identify lesions with FFR <0.80 (AUC 0.39, p=0.09), (sensitivity – 58% and specificity – 26% at a QCA stenosis of 50%). In contrast, 1D-vFFR had a better correlation with FFR (r=0.32, p=0.01) and significantly better diagnostic performance (AUC 0.67, p=0.007), (sensitivity – 92% and specificity - 29% at a 1D-vFFR of 0.7). Conclusions: 1D-vFFR improves the determination of functionally significant coronary lesions compared with conventional angiography without requiring a pressure-wire or hyperaemia induction. It is fast enough to influence immediate clinical decision-making but requires further clinical evaluation.

Diagnostic Performance of Virtual Fractional Flow Reserve derived from routine Coronary Angiography using Segmentation Free Reduced order (1-Dimensional) Flow Modelling

INTRODUCTION

Fractional flow reserve (FFR) is defined as the ratio of the mean distal coronary pressure (Pd) measured with a pressure wire to the mean proximal coronary pressure (Pa) measured at the guide catheter during maximum hyperaemic flow, usually achieved after bolus infusion of a pharmacological agent such as adenosine. The accuracy of FFR as an index of myocardial ischemia is validated and widely accepted (1-4). FFR-guided PCI improves patient outcomes, reduces number of stent insertions and lowers cost of treatment (1). However, it is used in <10% of PCI procedures even in the UK (5) and less than 40 % in European countries where the leaders in 2015 were Denmark (31%) and Belgium (29%) (6, 7), likely in part due to the additional time and cost incurred in performing invasive FFR.

Virtual FFR represents a novel, non-invasive method to assess FFR of a coronary artery lesion without the practical difficulties that limit the invasive technique. Recently, several virtual FFR methods have used full 3D segmentation and 3D computational fluid dynamics simulations. These take time, entail significant cost and require expertise in image-based computational fluid dynamics (CFD) coupled with either CT coronary angiograms or invasive rotational coronary angiography to calculate FFR without insertion of a pressure wire or use of pharmacological agents (8-12). With a view to reducing some of the above constraints, several groups are exploring simpler ‘reduced-order’ virtual FFR methods that involve 1D simulations, but still use a 3D segmentation to generate the 1D geometry (10, 11).

The aim of this study is to investigate whether useful virtual FFR results can be obtained with a 1D model using only a few basic measurements of stenosis geometry obtained from routine coronary angiographic images. This will enable fast, low cost and viable results for immediate decision-making in the clinic or catheter laboratory without complex image segmentation or complex CFD software.

METHODS

Study Population

In this single centre retrospective study, we included subjects aged ≥18 years who were investigated for chest pain with coronary angiography, and in whom a coronary stenosis was detected and were subsequently investigated with an FFR measurement after obtaining informed consent. Patients with in-stent restenosis at the target vessel, previous bypass surgery, and diffuse coronary disease were excluded.

Coronary Angiography and Invasive FFR measurements

Diagnostic coronary angiography was performed using a 5F or 6F catheter according to local procedures. At least 2 orthogonal projections were acquired of all potential coronary stenosis. After heparin (70–100 IU/kg IV) administration, and intra-coronary nitrate to obtain maximum coronary vasodilatation a calibrated 0.014-inch “PressureWire” guide wire (St Jude Medical, USA) was introduced into the guiding catheter. The pressure wire was advanced into the guiding catheter until the

pressure transducer was just outside its tip, and the pressure measured by the sensor was then normalized to that of the guiding catheter. The wire was then advanced into the vessel, distal to the target coronary stenosis. FFR was calculated as the lowest ratio of distal coronary pressure divided by aortic pressure after achievement of maximal hyperaemia at the steady-state, obtained using adenosine administration. Maximal hyperaemia was assumed after at least 1 minute in the presence of stable systemic blood pressure, decreased compared with baseline, remaining for at least 10 beats (13).

Quantitative Coronary Angiography

Quantitative assessment of stenosis severity at coronary angiography was performed offline and independently by two cardiologists using two-dimensional Quantitative Coronary Angiography (QCA) with a computer assisted automatic arterial contour detection system (Centricity CA-1000, GE Healthcare, Little Chalfont, United Kingdom) in the end-diastolic angiographic image, with optimal projection showing minimal foreshortening of the lesion. The software utilizes measurement calibration by comparing it with an object of known dimension and allows rapid quantification of vessel size and lesion length.

The cardiologists were blinded to clinical and hemodynamic data. Pixel size was determined with automated distance calibration and all analyses were performed on frames demonstrating optimal luminal opacification. The proximal and distal limits of the lesion were defined by manual inspection (corresponding to the sites of minimal luminal encroachment i.e., mean 10% diameter decrease compared with the reference vessel). The automated edge-detection software was then used to trace the lesion contours and determined the reference vessel diameter and luminal

diameter at maximal obstruction. Reference vessel diameter (RVD), lesion length (LL), minimal lumen diameter (MLD), and percentage diameter stenosis (DS) were calculated.

Calculation of 1D FFR:

Patient specific data to calculate an estimate of flow rate

For all patients height and weight were recorded and a value of body surface area (BSA) calculated (14). To avoid the need for additional invasive measurements a number of assumptions were applied. From the BSA, cardiac output was approximated based on an assumed cardiac index of 3 L/min/m^2, derived from healthy subjects >60 years old using cardiac magnetic resonance imaging (15). A coronary flow reserve of 3 was assumed, based on data in human subjects presenting with chest pain and who had angiographically normal coronary arteries (16). Based on the estimated cardiac output, estimated total coronary blood flow was derived from an assumed myocardial mass based on the relationship between normalized proximal arterial diameters and myocardial mass for different segments of LAD, LCX and RCA (17). Vessel-specific baseline coronary flow was then assumed to be proportional to subtended myocardial mass, based on an allometric scaling principle (17-21). Cross-sectional areas of LCA and RCA were calculated from LCA and RCA measurements, then allometric scaling was carried out by initially calculating flow through the left main coronary artery, assuming flow is divided between LCA and RCA in proportion to their areas. The coronary flow in the stenotic branch was calculated based on the area ratio of the stenotic branch to the left main coronary artery. An estimate of the hyperaemic flow was then derived from which a mean flow rate in the vessel of interest was obtained. We assumed that the increase

in flow under hyperaemic conditions is proportional to the resting flow, by reducing coronary resistance by a factor of 0.22, corresponding to a 3.5-fold increase in flow with respect to resting conditions (22). The performance of these modelling assumptions was further tested by re-analysing all results using other possible parameters but none achieved a better diagnostic accuracy (supplementary material).

1D computational flow analysis

The coronary geometrical data was extracted offline from 2-dimensional coronary angiograms using QCA. The extracted data (Reference vessel diameter (RVD), lesion length (LL), minimal lumen diameter (MLD), and percentage diameter stenosis (DS) was then combined with the estimated patient specific coronary flow rate calculated above and was incorporated into the 1D model containing wave speeds, material properties of the arteries and boundary conditions. Our code then generates the mesh to be introduced for analysis (24). This creates estimates of pressure (PD and PA) from which 1D-vFFR can be derived (Figure 1). The model uses established methods described extensively previously (23-25).

A coronary artery is represented as single segment, split into three parts, proximal part, stenosis and distal part is represented individually as one-dimensional (1D) segments, described by the equations of fluid flow and an equation governing the non-linear pressure-area elasticity relation. The coronary stenosis was represented with the lumped parameter stenosis model described by Young and Tsai (26), which contains empirically validated coefficients derived from stenosis length and relative diameter. Based on preliminary studies, the main determinant of FFR in such models is the flow through the stenosis. A representative coronary flow waveform was

prescribed at the inlet, while the patient-specific mean flow passing through the stenosis was estimated as described above.

Statistical Analysis

Statistical analysis was performed using the Statistical Package for the Social Sciences (SPSS 23.0, IBM Corp., Armonk, New York, USA). The correlation (Pearson) of both 1D-vFFR and QCA were compared to FFR. The diagnostic accuracy of 1D-vFFR was compared with QCA and against pressure-derived FFR using point estimates of sensitivity and specificity, and area under the curve analysis from receiver-operator characteristic curves (ROC). Statistical significance was accepted at a value of $p < 0.05$.

RESULTS

The 85 patients included 62 males with mean age of 64 ± 9 years old. Baseline characteristics of all patients are shown in Table 1. Mean FFR was 0.84 (SD 0.07) and 32% of the stenoses had an FFR value <0.80, and hence underwent revascularization.

QCA revealed the mean percentage of coronary stenosis by area was 54% ± 16% and the mean lesion length 13 ± 7 mm. Once angiographic images of the coronary artery had been acquired calculation of the 1D-vFFR took less than 1 minute. Coronary stenosis (QCA) had a statistically significant but weak correlation with FFR (r=-0.2, p= 0.04) and poor diagnostic performance to determine lesions causing significant reductions in FFR (<0.80), (area under the receiver operator characteristic

curve (AUC) 0.39, p= 0.09). If a QCA area stenosis of 50% was taken as the cut off the sensitivity to detect a significant stenosis (FFR<0.8) was 58% and the specificity 26%. If a more severe QCA area stenosis of 70% is used, then the sensitivity decreases to 11% with an increase in specificity to 71%. Compared with QCA, 1D-vFFR had a stronger correlation with FFR (r=0.32, p=0.01). Although the correlation between 1D-vFFR and FFR was only modest, 1D-vFFR provided an improvement in diagnostic accuracy over QCA (Figure 2). Overall compared with QCA, it showed significantly better diagnostic performance (AUC 0.67, p=0.007) (Figure 3). Using a 1D-vFFR cut of 0.7 gave a sensitivity of 92% and a specificity of 29%.

DISCUSSION

QCA vs. 1D-vFFR

We found that QCA was poor at determining a functionally significant stenosis by FFR. A QCA stenosis cutoff of 50% had a sensitivity of only 58% to detect an FFR<0.80, in contrast, if 1D-vFFR was used with a cut off 0.75 then the sensitivity was 83%. If the more stringent 1D-vFFR cut off 0.70 is used, then the sensitivity goes up to 92%, specificity is 29%.

Computational based methods to derive FFR

Calculation of FFR derived from CTCA has been performed for some time using 3D models of the coronary tree and ventricular myocardium modelled from a mid-diastolic time point. The coronary tree is segmented into millions of separate finite elements and computational flow dynamics used to calculate the pressure loss at specific locations by solving the Navier-Stokes equations. However this is

computationally very demanding requiring export of the images to a specialist facility with a processing time of at least 24 hours. This derived FFR_{CT} (HeartFlowInc, California, US) had a sensitivity of 85% and specificity of 79% in intermediate (30%-70%) stenosis (27). If used as a "gatekeeper" pre catheter lab it has been shown to reduce the number of coronary angiograms showing non-significant disease without impacting on the number requiring PCI (28). FFR_{CT} does have some limitations; numerous artefacts may affect CTA interpretability including calcification, misalignment, motion, and increased image noise. These may affect the model accuracy, preventing the calculation of an FFR_{CT} in a third of cases in one study (29, 30).

Angiography based methods to derive FFR

Invasive angiography remains the most widely used modality to assess coronary anatomy and numerous methods have been used to attempt to derive a "virtual" FFR from the invasive angiogram. Morris et al described one technique that derives the CT 3D coronary model from angiography rather than CTCA (31). This initially included pulsatile coronary flow which complicates the computation further requiring more than 24 hours to complete, however a later iteration utilising a "pseudo-transient" model of coronary flow reduced this time to <4 minutes but currently requires invasively measured coronary microvascular resistance (32). Both these techniques require rotational angiography which is not widely available and reduces their applicability. Other models use 3D-QCA and simplified computational flow modelling to rapidly derive a virtual FFR (33, 34). The latter, QFFR was recently evaluated in the prospective, multi-centre FAVOR II trial where it demonstrated a sensitivity of 87% to detect invasive measured FFR positive lesions (33). Although

promising, the requirement for 3D QCA, a modality not widely available limits its current utility.

Potential of reduced order models

Reduced order models for coronary haemodynamics are attractive as they are very quick and can easily incorporate relevant anatomical information. A reduced-order model is used to calculate the pressure and flow distribution for each coronary tree. Subsequently, for each location along the coronary tree, we extract quantitative features describing the anatomy as well as the computed FFR value at that location. They have existed since the 1970s with Young and Tsai (26, 34) able to predict pressure drops within about 20% for a variety of flow conditions and stenosis geometries, including both symmetric and non-symmetric stenosis. Pellicano et al describe FFR_{angio} which utilises a hybrid reduced order formulation with reduced order modelling of coronary flow in healthy regions and a more complex model in coronary stenosis (35). In the recent FAST-FFR trial this demonstrated impressive sensitivity (94%) to detect invasive FFR measured coronary stenosis (36). The model only requires standard angiographic images and the computational processing time is less than 3 minutes, however, image segmentation is still required which is done by specialised software which is then manually corrected, for which the time required is not specified and accounted for as a limitation (36).

In this study we used a 1D model initially described by Mynard and Nithiarasu (37). Application of 1D models to coronary circulation have shown promising results using CTCA (36-38) but to date this study is first to determine FFR from a standard coronary angiogram using a purely 1D model without 3D segmentation.

Limitations

Several limitations should be acknowledged. Our results represent a retrospective, small single centre experience including 102 intermediate coronary stenoses only and hence needs confirmation with larger, prospective multi-centre studies. In addition, patients who had previously undergone revascularization via coronary artery bypass grafting (CABG) surgery or had re-stenosis lesions were excluded from the study; for that reason, the accuracy of 1DFFR in these populations remains unknown.

Although at a cut off of 0.75, 1D-vFFR achieved a good sensitivity (83%), good positive predictive value (74.7%) and accuracy (68.6%) it had a low negative predictive value (52.4%) and specificity (35%) which meant a high rate of false positive (64.5%). With a cut off of 0.70, 1D-vFFR showed a higher sensitivity (92%), comparable positive predictive value (74.1%), better accuracy (72%) and negative predictive value (60%), but lower specificity (29%) and higher false positives (71%). This is most likely due to the assumptions that are inevitably required for the approach that we adopted; for example, improved estimation of hyperaemic coronary blood flow may improve accuracy further. In addition, stenosis geometry was represented by only three parameters (reference vessel diameter, percent stenosis and stenosis length); although missing complex features of the geometry, this approach was intentionally adopted to avoid the complex and time-consuming 3D segmentation process.

CONCLUSION

1D-vFFR improves the determination of the functional significance of coronary lesions compared with conventional angiography. It is derived using routine angiographic data and does not require a pressure-wire or hyperaemia induction. Standard QCA is used and no specialised image segmentation is required meaning it is fast enough to influence immediate clinical decision making and simple enough to be easily incorporated in the clinical workflow. Whilst the high sensitivity achieved raises the possibility that positive invasive FFR may be predicted in patients with a low 1D-vFFR, future work is required to establish whether this approach could have clinical value.

DECLARATIONS AND CONFLICTS OF INTEREST

The authors declared no potential conflicts of interest with respect to the research, authorship, and/or publication of this article.

FUNDING

The authors received no financial support for the research, authorship, and/or publication of this article.

REFERENCES

1. Pijls NH, Fearon WF, Tonino PA Siebert U, Ikeno F, Bornschein B, van't Veer M, Klauss V, Manoharan G, Engstrøm T, Oldroyd KG, Ver Lee PN, MacCarthy PA, De Bruyne B; FAME Study Investigators. Fractional flow reserve versus angiography for guiding percutaneous coronary intervention in patients with multivessel coronary artery disease: 2-year follow-up of the

FAME (Fractional Flow Reserve Versus Angiography for Multivessel Evaluation) study. J Am Coll Cardiol. 2010 Jul 13;56(3):177-84.

2. Pijls NH, van Schaardenburgh P, Manoharan G, Boersma E, Bech JW, van't Veer M, Bär F, Hoorntje J, Koolen J, Wijns W, de Bruyne B.Percutaneous coronary intervention of functionally nonsignificant stenosis: 5-year follow-up of the DEFER Study. J Am Coll Cardiol. 2007 May 29;49(21):2105-11.

3. Tonino PA, De Bruyne B, Pijls NH, Siebert U, Ikeno F, van' t Veer M, Klauss V, Manoharan G, Engstrøm T, Oldroyd KG, Ver Lee PN, MacCarthy PA, Fearon WF; FAME Study Investigators. Fractional flow reserve versus angiography for guiding percutaneous coronary intervention.N Engl J Med. 2009 Jan 15;360(3):213-24.

4. De Bruyne B, Fearon WF, Pijls NH, Barbato E, Tonino P, Piroth Z, Jagic N, Mobius-Winckler S, Rioufol G, Witt N, Kala P, MacCarthy P, Engström T, Oldroyd K, Mavromatis K, Manoharan G, Verlee P, Frobert O, Curzen N, Johnson JB, Limacher A, Nüesch E, Jüni P; FAME 2 Trial Investigators. Fractional flow reserve-guided PCI for stable coronary artery disease.N Engl J Med. 2014 Sep 25;371(13):1208-17. doi: 10.1056/NEJMoa1408758. Epub 2014 Sep 1. Erratum in: N Engl J Med. 2014 Oct 9;371(15):1465.

5. Morris PD, van de Vosse FN, Lawford PV, Hose DR, Gunn JP. "Virtual" (Computed) Fractional Flow Reserve: Current Challenges and Limitations. JACC CardiovascInterv. 2015;8(8):1009–1017. doi:10.1016/j.jcin.2015.04.006

6. Tilsted HH, Ahlehoff O, Terkelsen CJ, Pedersen F, Özcan C, Jørgensen TH, Nielsen-Kudsk JE, Ravkilde J, Nissen H, Pedersen SA, Havndrup O, Lassen JF. Denmark: coronary and structural heart interventions from 2010 to 2015. EuroIntervention. 2017;13:Z17–Z20.
7. Desmet W, Aminian A, Kefer J, Dens J, Bosmans J, Claeys M, Dubois C, Gach O, Janssens L, Schroeder E, Vermeersch P, Carlier M, Benit E, Hanet C.. Belgium: coronary and structural heart interventions from 2010 to 2015. EuroIntervention. 2017;13:Z14–Z16.
8. Koo BK, Erglis A, Doh JH, Daniels DV, Jegere S, Kim HS, Dunning A, DeFrance T, Lansky A, Leipsic J, Min JK.. Diagnosis of ischemia-causing coronary stenoses by noninvasive fractional flow reserve computed from coronary computed tomographic angiograms. Results from the prospective multicenter DISCOVER-FLOW (Diagnosis of Ischemia-Causing Stenoses Obtained Via Noninvasive Fractional Flow Reserve) study. J Am Coll Cardiol, 58 (2011), pp. 1989–1997
9. Douglas PS, Pontone G, Hlatky MA, Patel MR, Norgaard BL, Byrne RA, Curzen N, Purcell I, Gutberlet M, Rioufol G, Hink U, Schuchlenz HW, Feuchtner G, Gilard M, Andreini D, Jensen JM, Hadamitzky M, Chiswell K, Cyr D, Wilk A, Wang F, Rogers C, De Bruyne B; PLATFORM Investigators. Clinical outcomes of fractional flow reserve by computed tomographic angiography-guided diagnostic strategies vs. usual care in patients with suspected coronary artery disease: the prospective longitudinal trial of FFRct: outcome and resource impacts study. Eur Heart J. 2015 Sep 1. pii: ehv444
10. Tu S, Barbato E, Köszegi Z, Yang J, Sun Z, Holm NR, Tar B, Li Y, Rusinaru D, Wijns W, Reiber JH. Fractional flow reserve calculation from 3-dimensional

quantitative coronary angiography and TIMI frame count: a fast computer model to quantify the functional significance of moderately obstructed coronary arteries. JACC Cardiovasc Interv. 2014 Jul;7(7):768-77.

11. Papafaklis MI, Muramatsu T, Ishibashi Y, Lakkas LS, Nakatani S, Bourantas CV, Ligthart J, Onuma Y, Echavarria-Pinto M, Tsirka G, Kotsia A, Nikas DN, Mogabgab O, van Geuns RJ, Naka KK, Fotiadis DI, Brilakis ES, Garcia-Garcia HM, Escaned J, Zijlstra F, Michalis LK, Serruys PW. Fast virtual functional assessment of intermediate coronary lesions using routine angiographic data and blood flow simulation in humans: comparison with pressure wire - fractional flow reserve. EuroIntervention. 2014 Sep;10(5):574-83.
12. Morris PD, Ryan D, Morton AC, Lycett R, Lawford PV, Hose DR, Gunn JP. Virtual fractional flow reserve from coronary angiography: modeling the significance of coronary lesions: result from the VIRTU-1 (VIRTUal Fractional Flow Reserve From Coronary Angiography) study. J Am Coll Cardiol Intv, 6 (2013), pp. 149–157
13. Pijls NH, Sels JW. Functional measurement of coronary stenosis. J Am Coll Cardiol. 2012;59:1045–1057.
14. Mosteller RD. Simplified Calculation of Body Surface Area. N Engl J Med 1987 Oct 22;317(17):1098 (letter)
15. Carlsson M, Andersson R, Bloch KM, Steding-Ehrenborg K, Mosén H, Stahlberg F, Ekmehag B, Arheden H. Cardiac output and cardiac index measured with cardiovascular magnetic resonance in healthy subjects, elite athletes and patients with congestive heart failure. J Cardiovasc Magn Reson. 2012 Jul 28;14:51.

16. Kern MJ, Bach RG, Mechem CJ, Caracciolo EA, Aguirre FV, Miller LW, Donohue TJ. Variations in normal coronary vasodilatory reserve stratified by artery, gender, heart transplantation and coronary artery disease. J Am Coll Cardiol. 1996;28:1154–1160.
17. Choy JS, Kassab GS. Scaling of myocardial mass to flow and morphometry of coronary arteries. J ApplPhysiol (1985). 2008 May;104(5):1281-6
18. Chareonthaitawee P, Kaufmann PA, Rimoldi O, Camici PG. Heterogeneity of resting and hyperemic myocardial blood flow in healthy humans. Cardiovasc Res.2001 Apr;50(1):151-61.
19. Cain P, Ahl R, HedstromE, UganderM, Allansdotter-Johnsson A, Friberg P, Arheden H. Age and gender specific normal values of left ventricular mass, volume and function for gradient echo magnetic resonance imaging: a cross sectional study. BMC Med Imaging. 2009;9(2).
20. Kim H, Vignon-Clementel I, Coogan J, Figueroa C, Jansen K, Taylor C. Patient-specific modeling of blood flow and pressure in human coronary arteries. Ann Biomed Eng. 2010;38:3195-3209.
21. Le HQ, Wong JT, Molloi S. Allometric scaling in the coronary arterial system. Int J Cardiovasc Imaging. 2008 Oct;24(7):771-81.
22. Wilson R, Wyche K, Christensen B, Zimmer S, Laxson D. Effects of adenosine on human coronary arterial circulation. Circulation.1990;82:1595-1606.
23. Mynard JP, Penny DJ, Smolich JJ. Scalability and in vivo validation of a multiscale numerical model of the left coronary circulation. Am J Physiol Heart CircPhysiol 306: H517-H528, 2014.

24. Mynard JP, Smolich JJ. Influence of anatomical dominance and hypertension on coronary conduit arterial and microcirculatory flow patterns: A multi-scale modeling study. Am J Physiol Heart CircPhysiol 311: H11-H23, 2016.

25. Mynard JP, Nithiarasu P. A 1D arterial blood flow model incorporating ventricular pressure, aortic valve and regional coronary flow using the locally conservative Galerkin (LCG) method. CommNumer Methods Eng 24: 367-417, 2008.

26. Young DF, Tsai FY. Flow characteristics in models of arterial stenosis: II. Unsteady flow. J Biomech 6:547-559, 1973

27. Tonino PA, De Bruyne B, Pijls NH, Siebert U, Ikeno F, van' t Veer M, Klauss V, Manoharan G, Engstrøm T, Oldroyd KG, Ver Lee PN, MacCarthy PA, Fearon WF; FAME Study Investigators. Fractional flow reserve versus angiography for guiding percutaneous coronary intervention.N Engl J Med. 2009 Jan 15;360(3):213-24.

28. Nørgaard BL, Leipsic J, Gaur S, Seneviratne S, Ko BS, Ito H, Jensen JM, Mauri L, De Bruyne B, Bezerra H, Osawa K, Marwan M, Naber C, Erglis A, Park SJ, Christiansen EH, Kaltoft A, Lassen JF, Bøtker HE, Achenbach S; NXT Trial Study Group. Diagnostic performance of noninvasive fractional flow reserve derived from coronary computed tomography angiography in suspected coronary artery disease: the NXT trial (Analysis of Coronary Blood Flow Using CT Angiography: Next Steps).J Am CollCardiol. 2014 Apr 1;63(12):1145-1155. doi: 10.1016/j.jacc.2013.11.043. Epub 2014 Jan 30.

29. Douglas PS, De Bruyne B, Pontone G, Patel MR, Norgaard BL, Byrne RA, Curzen N, Purcell I, Gutberlet M, Rioufol G, Hink U, Schuchlenz HW, Feuchtner G, Gilard M, Andreini D, Jensen JM, Hadamitzky M, Chiswell K,

Cyr D, Wilk A, Wang F, Rogers C, Hlatky MA; PLATFORM Investigators. 1-Year Outcomes of FFRCT-Guided Care in Patients With Suspected Coronary Disease: The PLATFORM Study.J Am CollCardiol. 2016 Aug 2;68(5):435-445.

30. Lu MT, Ferencik M, Roberts RS, Lee KL, Ivanov A, Adami E, Mark DB, Jaffer FA, Leipsic JA, Douglas PS, Hoffmann U. Noninvasive FFR Derived From Coronary CT Angiography: Management and Outcomes in the PROMISE Trial.JACC Cardiovasc Imaging. 2017 Nov;10(11):1350-1358.
31. Morris PD, Silva Soto DA, Feher JFA, Rafiroiu D, Lungu A, Varma S, Lawford PV, Hose DR, Gunn JP. Fast Virtual Fractional Flow Reserve Based Upon Steady-State Computational Fluid Dynamics Analysis: Results From the VIRTU-Fast Study.JACC Basic Transl Sci. 2017 Aug 28;2(4):434-446.
32. Tu S, Barbato E, Köszegi Z, Yang J, Sun Z, Holm NR, Tar B, Li Y, Rusinaru D, Wijns W, Reiber JH. Fractional flow reserve calculation from 3-dimensional quantitative coronary angiography and TIMI frame count: a fast computer model to quantify the functional significance of moderately obstructed coronary arteries. JACC Cardiovasc Interv. 2014 Jul;7(7):768-77.
33. Westra J, Tu S, Winther S, Nissen L, Vestergaard MB, Andersen BK, Holck EN, Fox Maule C, Johansen JK, Andreasen LN, Simonsen JK, Zhang Y, Kristensen SD, Maeng M, Kaltoft A, Terkelsen CJ, Krusell LR, Jakobsen L, Reiber JHC, Lassen JF, Bottcher M, Botker HE, Christiansen EH, Holm NR. Evaluation of coronary artery stenosis by quantitative flow ratio during invasive coronary angiography: the WIFI II Study (Wire-Free Functional Imaging II). Circ Cardiovasc Imaging. 2018;11:e007107

34. Young DF, Tsai FY. Flow characteristics in models of arterial stenosis: I. Steady flow. J Biomech 6:395-410, 1973

35. Pellicano M, Lavi I, De Bruyne B, Vaknin-Assa H, Assali A, Valtzer O, Lotringer Y, Weisz G, Almagor Y, Xaplanteris P, Kirtane AJ, Codner P, Leon MB, Kornowski R. Validation Study of Image-Based Fractional Flow Reserve During Coronary Angiography. Circ Cardiovasc Interv. 2017 Sep;10(9). pii: e005259.

36. Fearon WF, Achenbach S, Engstrom T, Assali A, Shlofmitz R, Jeremias A, Fournier S, Kirtane AJ, Kornowski R, Greenberg G, Jubeh R, Kolansky DM, McAndrew T, Dressler O, Maehara A, Matsumura M, Leon MB, De Bruyne B; FAST-FFR Study Investigators. Accuracy of Fractional Flow Reserve Derived From Coronary Angiography. Circulation. 2019 Jan 22;139(4):477-484.

37. Mynard JP, Nithiarasu P. A 1D Arterial Blood Flow Model Incorporating Ventricular Pressure, Aortic Valve and Regional Coronary Flow Using Locally Conservative Galerkin (LCG) Method. Swansea University. Published in Communicating in Numerical Methods In Engineering, 2008; 24:367-417

38. Boileau E, Pant S, Roobottom C, Sazonov I, Deng J, Xie X, Nithiarasu P. Estimating the accuracy of a reduced-order model for the calculation of fractional flow reserve (FFR). Int J Numer Method Biomed Eng. 2018 Jan;34(1).

Figure Legends

Figure 1. Flow diagram showing the steps in creating the 1D-vFFR.

Table 1. Baseline characteristics of all patients are shown

Figure 2. (A) Positive stenosis by QCA (>70%) correctly predicts positive FFR (<0.80) with 1D-vFFR also positive (<0.75).

Figure 2. (B) Positive stenosis by QCA (>70%) provides a false positive reading as FFR is >0.80, 1D-vFFR (>0.75) correctly predicts lesion in not functionally significant.

Figure 3. Receiver Operator Characteristics (ROC) Curves comparing the diagnostic utility of mean area stenosis (derived from Quantitative Coronary Analysis (QCA)) and 1D-vFFR.

Supplementary Material

Diagnostic Performance of Virtual Fractional Flow Reserve derived using different modelling assumptions

Sensitivity of the diagnostic performance to the modelling assumptions used to derive 1D-vFFR was tested by analysing all results with the following alternative assumptions:

1) Representing the stenosis as a uniform one-dimensional segment with a length equal to stenosis length and diameter equal to minimal stenosis diameter, instead of the empirical model described by (Young and Tsai, 1973).
2) Assuming a cardiac index of 2.2 L/min/m^2 instead of 3 L/min/m^2.
3) Assuming a coronary flow reserve of 4 instead of 3.
4) Assuming a fixed total coronary flow of 3.8 mL/s, rather than estimating this flow based on body surface area, assumed cardiac index and 4% of cardiac output supplying the coronary circulation.
5) Assuming that the flow split at junctions is determined according to radius to the power of 3 or 2.7, rather than 2.

A total of 9 sets of simulations were performed with various combinations of these assumptions, where Model 1 refers to the model presented in the main manuscript. The results of all models are shown below in the Supplementary Table. These revealed a lower sensitivity to the modelling assumption employed, with the correlation coefficient between FFR and 1D-vFFR differing by less than 0.12 and the AUC differing by less than 0.04 in all cases tested.

Supplementary Table 1. Sensitivity to modelling assumptions

Method	Stenosis Model	CI	TCF	Radius exponent	CFR	R	AUC
1	YT	3	BSA	2	3	0.32	0.67
2	YT	-	3.8 mL/s	2	3	0.29	0.65
3	YT	3	BSA	2	4	0.31	0.66
4	YT	3	BSA	3	4	0.20	0.66
5	YT	3	BSA	2.7	4	0.23	0.67
6	1D	2.2	BSA	2	3	0.26	0.69
7	1D	3	BSA	2	3	0.27	0.69
8	1D	3	BSA	2	4	0.28	0.69
9	1D	-	3.8 mL/s	2	4	0.28	0.69

Abbreviations: 1D, stenosis represented as uniform one-dimensional segment with length and diameter derived from stenosis geometry; AUC, area under the curve; BSA, total coronary flow estimated from body surface area, cardiac index and assuming total coronary flow is 4% of cardiac output; CFR, coronary flow reserve; CI, cardiac index; R, Pearson's correlation coefficient; TCF, total coronary flow; YT, empirical stenosis model described by Young and Tsai (1973).

Mean Age, years	64(9)
Male, n	62
BMI, kg/m2	28.3(4)
Coronary arteries, n	
RCA	19
PDA	1
LMS	1
LAD	67
LCX	11
D1	1
OM1	2
QCA Mean coronary stenosis area,%	54 (16)
Coronary stenosis diameter/mm	1.31(0.5)
QCA Mean coronary stenosis diameter,%	44(12)
QCA Mean lesion length, mm	13 (7)

Table 1. Baseline characteristics of all patients (n=85)

BMI: body mass index, RCA: right coronary artery, PDA: posterior descending artery, LMS: left main stem, LAD: left anterior descending, LCX: left circumflex artery, D1: first diagonal branch, OM1: first obtuse marginal branch, QCA: quantitative coronary angiography.

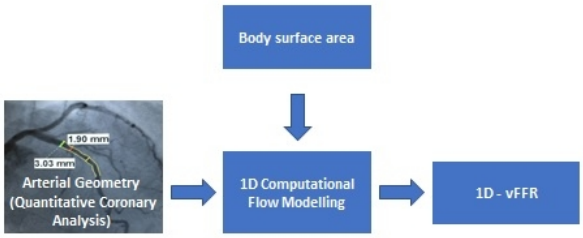

Figure 1. Flow diagram showing the steps in creating the 1D-vFFR.

203x162mm (96 x 96 DPI)

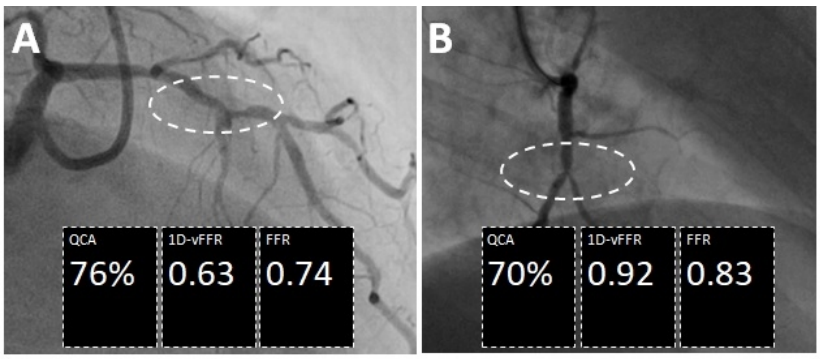

Figure 2. (A) Positive stenosis by QCA (>70%) correctly predicts positive FFR (<0.80) with 1D-vFFR also positive (<0.75).
Figure 2. (B) Positive stenosis by QCA (>70%) provides a false positive reading as FFR is >0.80, 1D-vFFR (>0.75) correctly predicts lesion in not functionally significant.

203x162mm (96 x 96 DPI)

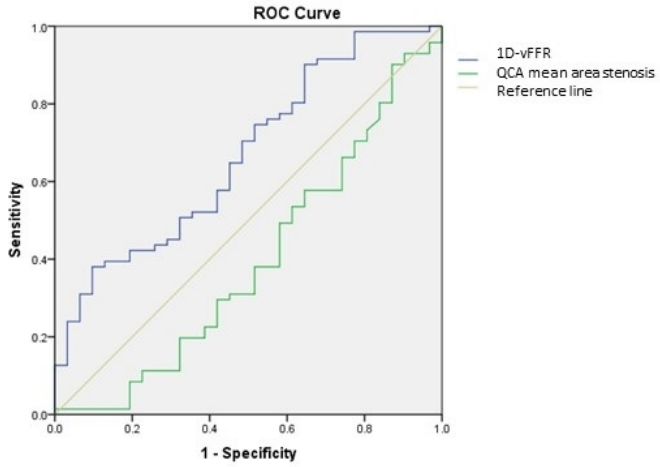

Figure 3. Receiver Operator Characteristics (ROC) Curves comparing the diagnostic utility of mean area stenosis (derived from Quantitative Coronary Analysis (QCA)) and 1D-vFFR.

203x162mm (96 x 96 DPI)